$(TTF)Pb_2I_5$: a Radical Cation-Stabilized Hybrid Lead Iodide with Synergistic Optoelectronic Signatures

Hayden A. Evans,[†,‡,§] Anna J. Lehner,[§] John G. Labram,[∥] Douglas H. Fabini,[§,⊥] Omar Barreda,[§] Sara R. Smock,[‡] Guang Wu,[‡] Michael L. Chabinyc,[∥,⊥*] Ram Seshadri,[†,‡,§,⊥*] and Fred Wudl[‡,§,⊥*]

[†]Mitsubishi Chemical Center for Advanced Materials, University of California, Santa Barbara, CA 93106

[‡]Department of Chemistry and Biochemistry, University of California, Santa Barbara, CA 93106

[§]Materials Research Laboratory, University of California, Santa Barbara CA 93106

[∥]California NanoSystems Institute, University of California, Santa Barbara CA 93106

[⊥]Materials Department, University of California, Santa Barbara, CA 93106, USA.

ABSTRACT: Hybrid organic–inorganic materials offer the opportunity to combine functionalities of two distinct chemistries. Tetrathiafulvalene (TTF) is the precursor to some of the first organic metals, and perovskite lead iodides have recently proved their efficacy as photovoltaic materials. Here we describe a hybrid material that incorporates both, comprising TTF radical cations stabilizing an anionic layered lead–iodide network. Preparation, property analysis, and DFT calculations are reported, verifying that $(TTF)Pb_2I_5$ is a narrow gap semiconductor with optical properties synergistically influenced by the $TTF^{+\bullet}$ radical cation. This radical cation contributes to states in the electronic gap formed by orbitals in the inorganic framework.

Hybrid organic-inorganic materials can potentially combine the properties of highly tunable functional organics with those of complementary inorganic networks in a single material. Distinct control over what is desired from each component becomes possible in such materials, allowing the functions of the organic and inorganic components to work synergistically. Tetrathiafulvalene (TTF), the organic component in the new hybrid material reported here, is a precursor to some of the early organic metals and was a clear choice when choosing a functional organic. It was first reported by Wudl *et al.* in the early 1970's,[1,2] and has been studied for its impressive electron donating abilities,[3,4] including derivatives displaying superconductivity.[5]

Hybrid compounds containing TTF have also shown novel electronic and magnetic properties. Devic *et al.*[6,7] reported a ethylenedithio-1,2-diiodotetrathiafulvalene ($EDT\text{-}TTF\text{-}I_2^{+\bullet}$) hybrid with metallic character, and showed its metal-insulator transition to be preserved within a hybrid compound with PbI_2. Kondo *et al.*[8] similarly reported $TTF^{+\bullet}$ hybrids containing Sn and Cl/Br, all which display semiconducting behavior due to interactions through the extended TTF networks. Magnetic compounds with TTF derivatives have also been made with transition metal halides, and found to be composed of two kinds of donor columns which magnetically couple with the anions through close contact between metal halide interactions.[9] Metal-organic-frameworks (MOFs), a related class of hybrid materials, generally possess poor electronic functionality, but attempts to prepare electrically conductive MOFs have recently been made. Examples include incorporating a conjugated molecule within the framework directly,[10] as a guest that electronically couples metal atoms in the framework using (TCNQ),[11] or post-synthetic modification of an insulating MOF via chemical leaching.[12,13] Stavila *et al.*[14] have recently reviewed this topic.

Layered lead halides, in their own right, are an attractive set of materials with rich optoelectronic and semiconducting behavior. The extensive work of Mitzi and coworkers[15,16] in the late 90's first highlighted how amines and diammines combine with main group halides to form unique layered perovskite structures, which motivated the chemistry of organic ammonium cation "spacers" to flourish. Following the work of Kojima *et al.*[17] demonstrating the use of perovskite $CH_3NH_3PbI_3$ materials as solution deposited photovoltaics, there has been a huge flurry of research in this space to enhance the stability of the air unstable compound. This has included the use of ammonium "spacer" chemistry by Smith *et al.*[18] which improved stability of a layered perovskite incorporating phenylethylammonium ions into the structure. Cao *et al.*[19] also explored this idea with butylammonium instead of phenylethylammonium, and reported that the extent of ammonium spacer incorporation as well as growth direction of subsequent films had significant im-

pact on functionality of their light absorbing devices. Maughan *et al.*[20] recently highlighted how the unusual aromatic cation tropylium^{+} can stabilize and electronically couple with tin and lead halide networks, helping to defining the position of either the conduction band maximum or valence band minimum.

Here we report a semiconducting hybrid compound with radical cation $TTF^{+\bullet}$ stacks that separate condensed $Pb_2I_5^-$ slabs in a manner that allows both the organic and the inorganic components of the hybrid to play an electronic role. $(TTF)Pb_2I_5$ crystals were grown under argon atmosphere by dissolving PbI_2 (110 mg, 0.239 mmol) and tetrabutylammonium iodide (168.2 mg, 0.455 mmol) in dimethylformamide (DMF, 1 cm^3) at ambient temperature. Following complete dissolution, a separate solution of $(TTF)_3(BF_4)_2$ (20 mg, 0.0254 mmol) prepared following the literature procedure,[21] in DMF (3 cm^3) was added drop-wise. The resulting mixture is dark with red hue. This mixture was layered with acetonitrile (CH_3CN, 6 cm^3) as non-solvent and left at room temperature for 2 days. Small dark bundles of crystals were formed beneath an unreacted PbI_2 layer. These bundles were isolated by washing with cold DMF, air dried, and finally dried in vacuum. The dark crystal bundles, when broken up, yield red rectangular single crystals. The material was observed stable in air for a month, but longer time study is needed.

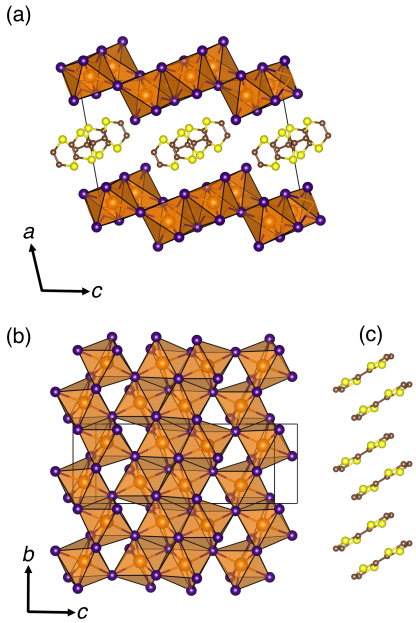

Figure 1. The crystal structure of the title compound $(TTF)Pb_2I_5$. (a) View down the *b* axis showing the corrugated $Pb_2I_5^-$ layers. (b) A top view of the lead iodide layers, showing both edge and corner sharing of the octahedra. (c) $TTF^{+\bullet}$ radical cations extend infinitely in stacks, with complete overlap as dimers, and partial overlap with the next nearest neighbor dimer pair. Space group $P2_1/c$, a = 12.90(3) Å, b = 7.97(1) Å, c = 20.23(2) Å, β = 100.25(7)°, Z= 4 R_1 = 1.695 %, wR_r = −1.591 %.

Single crystal X-ray diffraction carried out on multiple crystals confirmed the structure depicted in Figure 1(a). Figure 1(a) illustrates different views of the $(TTF)Pb_2I_5$ structure with some crystallographic details in the caption. The structure comprises sheets of corner and edge sharing lead iodide octahedra, separated by $TTF^{+\bullet}$ cations that form stacks perpendicular to the anionic slabs. The $TTF^{+\bullet}$ stacks contain eclipsed dimers (two $TTF^{+\bullet}$) and maintain a consistent intra-dimer distance of 3.32 Å. The stacks extend through the crystal with an incomplete overlap with the next nearest TTF pairs, with an inter-dimer distance of 3.52 Å, as shown in Figure 1(c). It is interesting to note that this stacking structure of the TTF radical cations is commensurate with the corrugated sheet structure of the Pb-I sheets. In contrast to the previous work on EDT-TTF-I_2 iodoplumbates reported by Devic *et al.*,[6] there is no disorder of the radical cation, which were reliably located over the temperature range of 373 K to 100 K. There is a slight contraction of the unit cell at 100 K, but no structural transition was observed in this temperature range.

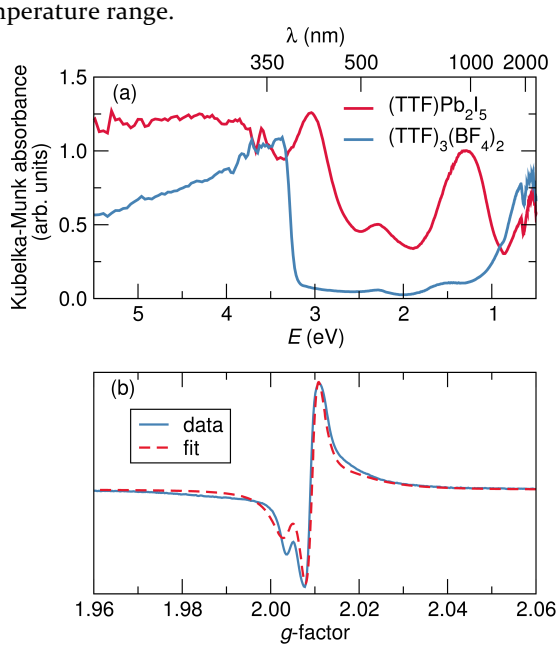

Figure 2. (a) Kubelka-Munk absorbance obtained from transformation of the diffuse reflectance UV-Vis spectra of $(TTF)Pb_2I_5$, as well as the precursor salt $(TTF)_3(BF_4)_2$. (b) Room-temperature ESR signal of polycrystalline $(TTF)Pb_2I_5$ sample, 9.2898 GHz, shown along with the simulation using *g* values of 2.0110, 2.0083, and 2.053.

Figure 2(a) displays UV-Vis spectra obtained for $(TTF)Pb_2I_5$, as well as the starting material, $(TTF)_3(BF_4)_2$. The spectra were obtained using a Shimadzu UV3600 UV-NIR Spectrometer in diffuse reflectance mode using an integrating sphere and relative absorbance was obtained from Kubelka-Munk transformation of the reflectance spectra. Samples were diluted with $BaSO_4$ prior to measurement. Prior work from Sugano *et. al*[22] and Torrance *et. al*[23,24] were the main sources used for interpreting the presented spectra. The insulating TTF salt, $(TTF)_3(BF_4)_2$, has

a structure comprising dimers and neutral TTF that are staggered with distances varying between 3.4 Å and 3.48 Å.[25] We observe noticeable absorptions for this salt near 0.6 eV which are attributed to intermolecular charge transfer from TTF^0 to $TTF^{+\bullet}$, as well as an absorption attributed to an *intra*molecular transition for a lone $TTF^{+\bullet}$ within a dimer at 3.18 eV.[22,24] The weak peaks at 1.5 eV and 2.3 eV are an intradimer transition and an intramolecular $TTF^{+\bullet}$ transition, respectively.[24]

Considering what is already known for monovalent and mixed valence $TTF^{+\bullet}$ salts the absorption spectra of the title compound is not surprising. The broad band that peaks near 1.3 eV is from intradimer charge transfer, and the absorptions that peak at 2.3 eV and 3.0 eV are intramolecular transitions of the $TTF^{+\bullet}$. What is unexpected however, is the low energy absorption at 0.6 eV which is attributed to *inter*molecular charge transfer from TTF^0 to $TTF^{+\bullet}$. Although no crystallographically observed TTF^0 is present in our sample, we believe the cause of this absorption is back charge transfer from the Pb-I network to $TTF^{+\bullet}$, in a manner similar to how $TCNQ^{-\bullet}$ back charge transfers to NMP^+ in NMP–TCNQ.[23] Furthermore, the sustained absorption over the 3.0 eV to 5.5 eV range is not usually seen for $TTF^{+\bullet}$ salts, which we attribute to absorption from the Pb-I network.

Figure 2(b) displays Electron spin resonance (ESR) spectra of powder samples of $(TTF)Pb_2I_5$, providing evidence of the radical cation state of $TTF^{+\bullet}$ at room temperature. The signal is centered close to the value for a free electron with an asymmetrical signal shape suggestive of some itinerant electron character, consistent with the observed free-carrier behavior.[26] The simulation of the EPR spectrum, which is depicted in Figure 2(b) as a dashed line, was carried out using Easy Spin[27] (details in SI).

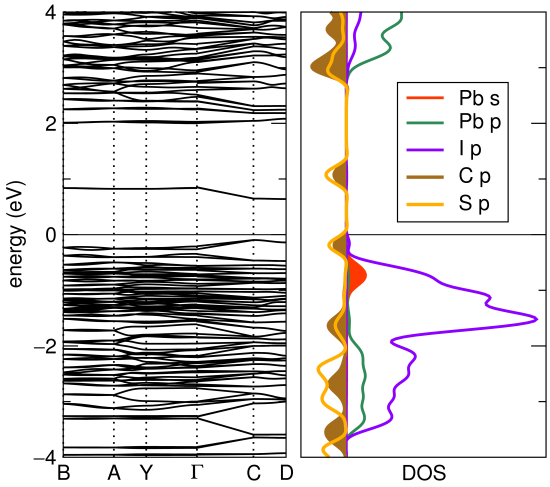

Figure 3. Band structure (PBE) and DOS (HSE06) for $(TTF)Pb_2I_5$. The DOS contributions of the C and S p states from $TTF^{+\bullet}$ and the Pb and I contributions have been separated for added clarity.

Band structure calculations of $(TTF)Pb_2I_5$ based on density functional theory (DFT) were carried out using the Vienna ab initio Simulation Package (VASP)[28–31] which implements the Kohn-Sham formulation using a plane wave basis and the projector-augmented wave formalism (PAW).[32,33] The input structure was generated from the single crystal diffraction data by adding the aromatic H atoms to the $TTF^{+\bullet}$ radical cation and constraining them within the normal riding model of the HFIX function of the crystallographic refinement software SHELXL-2014.[34,35] We decided to use this input model without any DFT structure optimization as the relaxed structure exhibited an increased volume (9 %) and considerable deviations in polyhedral volumes for the complex Pb–I anions compared to the crystallographic results, potentially as a result of van der Waals interactions not being appropriately captured. The energy cut-off of the plane wave basis set was 500 eV and a Γ-centered *k*–mesh grid with 24 *k*–points was employed, with the convergence criteria set at 0.01 meV. The Perdew-Burke-Ernzerhof (PBE)[36] version of the Generalized Gradient Approximation for employed for the exchange-correlation energy. The high-symmetry points were selected for the conventional Brillouin zone of the space group $P2_1/c$ using the Bilbao Crystallographic Server.[37] For more accurate band gap values and density of states (DOS), a screened hybrid functional (HSE06)[38,39] was employed. Spin-orbit coupling (SOC), which we found to be necessary to accurately describe the band structures of related lead[40] and bismuth[41] halides was not employed in the results presented here: SOC affects only impacts the band dispersion of the Pb states, which do not contribute significantly to the states around the band gap in $(TTF)Pb_2I_5$. For comparison, the electronic structure of $TTFI_3$[42] ($P2_1/n$) was calculated using the same computational scheme, and is provided in the Supporting Information. The calculated band gap (HSE-level) of 1.02 eV is indirect between the valence band maximum (VBM, C) and the conduction band minimum (CBM, D) and corresponds to a transition between filled and empty sulfur p and carbon p states. Its magnitude is only marginally smaller than the smallest direct transition (1.03 eV) which is located at the special *k* point C.

We find the states of the $TTF^{+\bullet}$ radical cation to be energetically surrounded by filled states of the antibonding interaction between the lone-pair Pb s^2 states with the halogen p states in the valence band and by empty Pb p states in the conduction band. In other hybrid lead halides with simple aliphatic carbon hydrate counter cations, such as $CH_3NH_3PbI_3$, the filled counter-cation states are energetically far below the Fermi energy and the surrounding Pb-I states constitute the VBM and CBM. The band dispersion of the $TTF^{+\bullet}$ states around the band gap is relatively moderate, as would be expected of the 1D stacks.

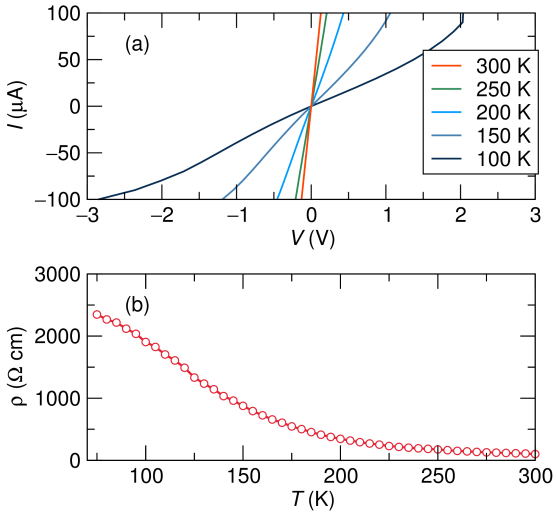

Figure 4. Four-probe measurements for $(TTF)Pb_2I_5$. (a) IV characteristics over the 100 K to 300 K range. (b) ρ *vs. T* between 75 K and 300 K. The room temperature resistivity of the pressed pellet is close to 100 Ω cm.

Four-probe electrical resistivity measurements were carried out on a pressed pellet of polycrystalline $(TTF)Pb_2I_5$ with evaporated gold contacts (schematic shown in the SI). Figure 4(a) shows *I–V* curves from 100 K to 300 K, suggesting nearly Ohmic behavior near the origin. As can be seen from Figure 4(b), as temperature is increased from 75 K to 300 K the resistivity of $(TTF)Pb_2I_5$ decreases by two orders of magnitude. The conductivity of the pressed pellet of the title compound is considerably higher than related monocation salts $[(TTF)Br_{1.0}$ and $(TTF)Cl_{1.0}]$ which have conductivities close to 10^{-6} S cm^{-1} when measured similarly.[43] We believe the increased conductivity can be attributed to the synergistic effect of the inorganic network.

In summary, we have isolated a $TTF^{+\bullet}$ radical cation stabilized iodoplumbate that displays semiconducting behavior, with a room-temperature resistivity close to 100 Ω cm (conductivity greater than 0.01 S cm^{-1}). The electronic and optical properties of the compound are greatly influenced by the $TTF^{+\bullet}$ radical cation, which creates states in the electronic gap formed by the lead-iodide matrix. We believe these types of synergistic hybrid systems to be potentially promising materials as next generation photovoltaic materials and other optoelectronic applications, that encourages further exploration.

ASSOCIATED CONTENT

Supporting Information

TGA, PXRD, and crystallographic information including `.cif` of $(TTF)Pb_2I_5$. DOS structure and the methods used for related $(TTF)I_3$ compound. The Supporting Information is available free of charge on the ACS Publications website.

AUTHOR INFORMATION

Corresponding Authors

mchabinyc@engineering.ucsb.edu, seshadri@mrl.ucsb.edu, wudl@chem.ucsb.edu

ACKNOWLEDGMENT

This work was supported by the U.S. Department of Energy, Office of Science, Basic Energy Sciences under Award No. DE-SC-0012541. A.J.L. gratefully acknowledges support of Swiss National Science Foundation Fellowship No. PBSKP2-145825. O.B. gratefully acknowledges RISE Program for support. The research involved the use of shared experimental facilities of the Materials Research Laboratory and the Center for Scientific Computing at UCSB supported by the MRSEC Program of the National Science Foundation under Award Nos. DMR 1121053 and NSF CNS-0960316.

REFERENCES

1. Wudl, F.; Smith, G. M.; Hufnagel, E J. Unusually Stable Organic Radical. *Chem. Commun.* **1970**, 1453–1454.
2. Wudl, F.; Wobschall, D.; Hufnagel, E. Electrical conductivity by the bis (1, 3-dithiole)-bis (1, 3-dithiolium) system. *J. Am. Chem. Soc.* **1972**, *94*, 670–672.
3. Bryce, M. R. Functionalized tetrathiafulvalenes: new applications as versatile π-electron systems in materials chemistry. *J. Mater. Chem*, **2013**, *10*, 589–598.
4. Martin, N. Tetrathiafulvalene: the advent of organic metals. *Chem. Commun.*, **2013**, *49*, 7025–7027.
5. Crabtree, G. W.; Carlson, K. D.; Hall, L. N.; Copps, P. T.; Wang, H. H.; Emge, T. J.; Beno, M. A.; Williams, J. M. Superconducvitity at ambient pressure in di{bis{ethyleledithio)tetrathiafulvalene]triiodide, (BEDT)-$TTF)_2I_3$. *Phys. Rev. B.*, **1984**, *30*, 2958–2960.
6. Devic. T.; Evain, M.; Moëlo, Y.; Canadell, E.; Auban-Senzier, P.; Fourmigué, M.; Batail, P. Single crystalline commensurate metallic assemblages of π-slabs and CdI_2-type layers: synthesis and properties of β-(EDT-TTF-$I_2)_2[Pb_{5/6}\square_{1/6}I_2]_3$ and β-(EDT-TTF-$I_2)_2[Pb_{2/3+x}Ag_{1/3-2x}\square_xI_2]_3$, x=0.05. *J. Am. Chem. Soc.* **2003**, *125*, 3295–3301.
7. Devic, T.; Canadell, E.; Auban-Senzier, P.; Batail, P. (EDT-TTF-$I_2)_2PbI_3$•H2O: an ambient pressure metal with a β' donor slab topology. *J. Mater. Chem*, **2004**, *14*, 135–137.
8. Kondo, K.; Matsubayashi, G.; Tanaka, T. Preparation and properties of tetrathiafulvalene (ttf) and tetramethyltetraselenafulvalene salts of tin(IV) halide anions and X-ray crystal structure of $[TTF_3[SnCl_6]$. *J. Chem. Soc. Dalton Trans.* 1984, *3*, 379–384.
9. Kumai, R.; Asamitsu, A.; Tokura, Y. Magnetic and transport properties of organic radical ion salts containing tetrahalogenoferrate anion. *Synt. Met.*, **1997**, *85*, 1681–1682.
10. Narayan, T. C.; Miyakai, T.; Seki, S.; Dincă, M. High Charge Mobility in a Tetrathiafulvalene-Based Microporous Metal–Organic Framework. *J. Am. Chem. Soc.* **2012**, *134*, 12932–12935.
11. Talin, A. A.; Centrone, A.; Ford, A. C.; Foster, M. E.; Stavila, V.; Haney, P.; Kinney, R. A.; Szalai, V.; Gabaly, F. E.; Yoon, H. P.; Léonard, F.; Allendorf, M. D. Tuanable Electrical Conductivity in Metal–Organic Framework Thin–Film Devices. *Science* **2014**, *343*, 66–69.
12. Tominaka, S.; Hamoudi, H.; Suga, T.; Bennett, T. D.; Cairns, A. B.; Cheetham, A. K. Topochemical conversion of a dense metal–organic framework from a crystalline insulator to an amorphous semiconductor. *Chem. Sci.*, **2015**, *6*, 1465–1473.
13. Beldon, P.J.; Tominaka, S.; Singh, P.; Saha Dasgupta, T.; Bithel, E. G.; Cheetham, A. K. Layered structures

and nanosheets of pyrimidinethiolate coordination polymers. *Chem. Commun.* **2014**, *50*, 3955–3957.
14. Stavila, V.; Talin, A. A.; Allendorf, M. D. MOF-based electronic and optoelectronic devices. *Chem. Soc. Rev.* **2014**, *43*, 5994–6010.
15. Mitzi, D. B.; Field, C. A.; Harrison, W. T. A.; Guloy, A. M. Conducting tin halides with a layered organic-based perovskite structure. *Nature* **1994,** *369*, 467–469.
16. Mitzi, D. B.; Wang, S.; Field, C. A.; Chess, C. A.; Guloy, A. M. Conducting Layered Organic-inorganic Halides Containing <110>-Oriented Perovskite Sheets. *Science*, **1995**, *267*, 1473–1476.
17. Kojima, A.; Teshima, K.; Shirai, Y. Miyasaka, T. Organometal halide perovskites as visible-light sensitizers for photovoltaic cells. *J. Am. Chem. Soc.* **2009**, *131*, 6050–6051.
18. Smith, I. C.; Hoke, E. T.; Solis-Ibarra, D.; McGehee, M. D.; Karunadasa, H. I. A Layered Hybrid Perovskite Solar-Cell Absorber with Enhanced Moisture Stability. *Angew. Chem.* **2014**, *126*, 11414–11417.
19. Cao, D. H.; Stoumpos, C. C.; Farha, O. K.; Hupp, J. T.; Kanatzidis, M. G. Two-dimensional homologous perovskites as light absorbing materials for solar cell applications. *J. Am. Chem. Soc.* **2015**, *137*, 7843–7850.
20. Maughan, A. E.; Kurzman, J. A.; Neilson, J. R. Hybrid Inorganic–Organic Materials with an Optoelectronically Active Aromatic Cation: $(C_7H_7)_2SnI_6$ and $C_7H_7PbI_3$. *Inorg. Chem.*, **2015**, *54 (1)*, 370–378.
21. Wudl, F.; Kaplan, M. L.; Engler, E. M.; Patel, V. V. 2,2′-Bi-L,3-Dithiolylidene (Tetrathiafulvalene, Ttf) and its Radical Cation Salts. *Inorg. Synth.* **1979**, *19*, 27–34.
22. Sugano, T.; Yakushi, K.; Kuroda, H. Polarized Absorption Spectra of Single Crystals of Tetrathiafulvalenium Salts. *Bull. Chem. Soc. Jpn.* **1978**, *51*, 1041–1046.
23. Torrance, J. B.; Scott B. A.; Kaufman, F. B. Optical Properties of Charge Transfer Salts of Tetracyanoquinodimethane (TCNQ). *Solid State Commun.* **1975**, *17*, 1369–1373.
24. Torrance, J. B.; Scott, B. A.; Welber, B.; Kaufman, F. B.; Seiden, P. E. Optical properties of the radical cation tetrathiafulvalenium (TTF+) in its mixed-valence and monovalence halide salts. *Phys. Rev. B* **1979**, *19*, 730–741.
25. Legros, J-P.; Bousseau, M.; Valade, L.; Cassoux, P. Crystal Structure of a non-conductive Non-stoichiometric Tetrathiafuvalenium Salt: (TTF)3(BF4)2. *Mol. Cryst. Liq. Cryst.* **1983**, *100*, 181–192.
26. Wagoner, G. Spin Resonance of Charge Carriers in Graphite. *Phys. Rev.* **1960**, *118*, 647–653.
27. Stoll, S.; Schweiger, A. EasySpin, a comprehensive software package for spectral simulation and analysis in EPR. *J. Magn. Reson.* **2006,** *178*, 42-55.
28. Kresse, G.; Hafner, J. Ab Initio Molecular Dynamics for Liquid Metals. *Phys. Rev. B* **1993**, *47*, 558–561
29. Kresse, G.; Hafner, J. Ab Initio Molecular-Dynamics Simulation of the Liquid-Metal-Amorphous-Semiconductor Transition in Germanium. *Phys. Rev. B* **1994**, *49*, 14251–14269.
30. Kresse, G.; Furthmüller, J. Efficiency of Ab-Initio Total Energy Calculations for Metals and Semiconductors Using a Plane-Wave Basis Set. *Comput. Mat. Sci.* **1996**, *6*, 15–50.
31. Kresse, G.; Furthmüller, J. Efficient Iterative Schemes for ab Initio Total-Energy Calculations Using a Plane-Wave Basis Set. *Phys. Rev. B* **1996**, *54*, 11169–11186.
32. Blöchl, P. E. Projector Augmented-Wave Method. *Phys. Rev. B* **1994**, *50*, 17953–17979.
33. Kresse, G.; Joubert, D. From Ultrasoft Pseudopotentials to the Projector Augmented-wave Method. *Phys. Rev. B* **1999**, *59*, 1758–1775.
34. Sheldrick, G. M. *ShelXL-97 – Program for the Refinement of Crystal Structures*. University of Götteningen, Germany, 1997.
35. Sheldrick, G. M. A Short History of SHELX. *Acta Crystallogr. A* **2008**, *64*, 112–122.
36. Perdew, J.P.; Burke, K: Ernzerhof, M. Generalized Gradient Approximation Made Simple. *Phys. Rev. Lett.* **1996**, *77*, 3865–3868.
37. Aroyo, M. I.; Orobengoa, D.; de la Flor, G.; Perez-Mato, J. M.; Wondratschek, H. Brillouin-Zone Databases on the Bilbao Crystallographic Server. *Acta Crystallogr. A* **2014**, *70*, 126–137.
38. Heyd, J.; Scuseria, G. E.; Ernzerhof, M. Hybrid Functionals Based on a Screened Coulomb Potential. *J. Chem. Phys.* **2003**, *118*, 8207–8215.
39. Heyd, J.; Scuseria, G. E. Efficient hybrid density functional calculations in solids: Assessment of the Heyd–Scuseria–Ernzerhof screened Coulomb hybrid functional. *J. Chem. Phys.* **2004**, *121*, 1187–1192.
40. Brgoch, J.; Lehner, A. J.; Chabinyc, M.; Seshadri, R. Ab Initio Calculations of Band Gaps and Absolute Band Positions of Polymorphs of $RbPbI_3$ and $CsPbI_3$: Implications for Main-Group Halide Perovskite Photovoltaics. *J. Phys. Chem. C* **2014**, *118*, 27721–27727.
41. Lehner, A. J.; Wang, H.; Fabini, D. H.; Liman, C. D.; Hébert, C.-A.; Perry, E. E.; Wang, M.; Bazan, G. C.; Chabinyc, M. L.; Seshadri, R. Electronic Structure and photovoltaic application of BiI_3. *Appl. Phys. Lett.* **2015**, *107*, 131109–1–131109–4.
42. Teitelbaum, R. C.; Marks, T. J.; Johnson, C. K. A resonance Raman/iodine Moessbauer investigation of the starch-iodine structure. Aqueous solution and iodine vapor preparations. *J. Am. Chem. Soc.* **1980**, *102*, 2986–2989.
43. Scott, B. A.; LaPlaca, S, J.; Torrance, J.B., Silverman, B. D.; Welber, B. The crystal chemistry of organic metals. Composition, structure, and stability in the tetrathiafulvalinium-halide systems. *J. Am. Chem. Soc.* **1977**, *99*, 6631–6639

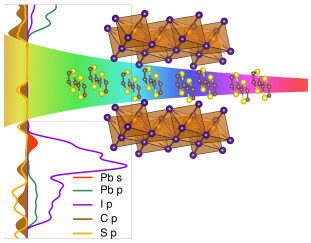
Pb s
Pb p
I p
C p
S p

Supporting Information for: (TTF)Pb_2I_5: a Radical Cation-Stabilized Hybrid Lead Iodide with Synergistic Optoelectronic Signatures

Hayden A. Evans,[†,‡,§] Anna J. Lehner,[§] John G. Labram,[‖] Douglas H. Fabini,[§,⊥] Omar Barreda,[§] Sara R. Smock,[‡] Guang Wu,[‡] Michael Chabinyc,[‖,⊥*] Ram Seshadri,[†,‡,§,⊥*] and Fred Wudl[‡,§,⊥*]

[†]Mitsubishi Chemical Center for Advanced Materials, University of California, Santa Barbara, California, 93106, United States

[‡]Department of Chemistry and Biochemistry, University of California, Santa Barbara, California, 93106, United States

§Materials Research Laboratory, University of California, Santa Barbara California, 93106, United States

‖California NanoSystems Institute, University of California, Santa Barbara, California, 93106, United States

⊥Materials Department, University of California, Santa Barbara, California, 93106, United States

TGA:

A TA Instruments Discovery TGA was utilized for the thermogravimetric analysis. A rate of 25 cm^3/min dry nitrogen purge was employed with a temperature ramp rate of 10°C/min. The maximum temperature of the experiment was 800°C.

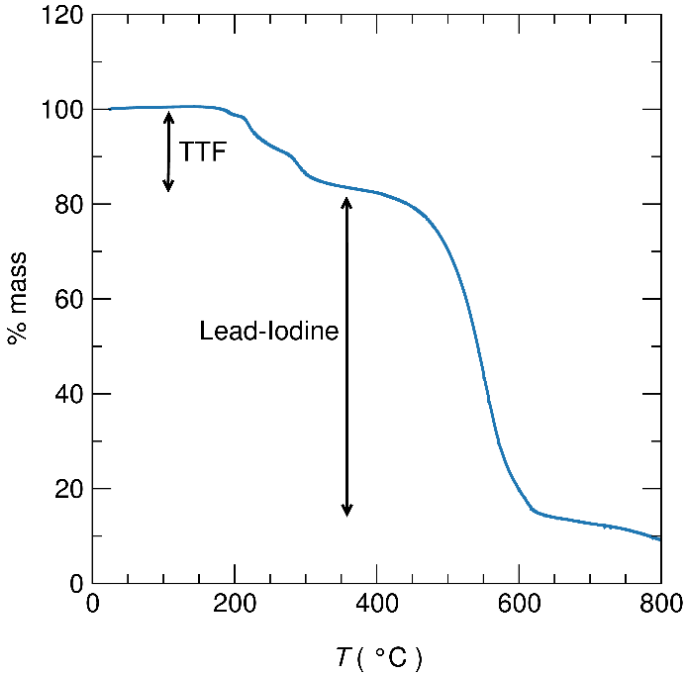

Figure S1. TGA data for the title compound (TTF)Pb_2I_5. The organic component (tetrathiafulvalene, TTF) is presumed to be the first part to degrade from the sample, at

temperatures beyond 200°C. This assertion agrees with the percent mass loss, matching the ~19% mass weight that TTF contributes to the (TTF)Pb_2I_5 formula weight.

Powder X-ray Diffraction (PXRD)

PXRD data was acquired on a Pananalytical Empyrean Powder XRD machine. PXRD data was utilized to establish bulk sample purity of isolated (TTF)Pb_2I_5 over the course of our experiments. We compared experimental PXRD with a simulated pattern generated from single crystal x-ray diffraction data, simulated with the program GSAS.[1,2] The data shown in Figure S2 was carried out open to air.

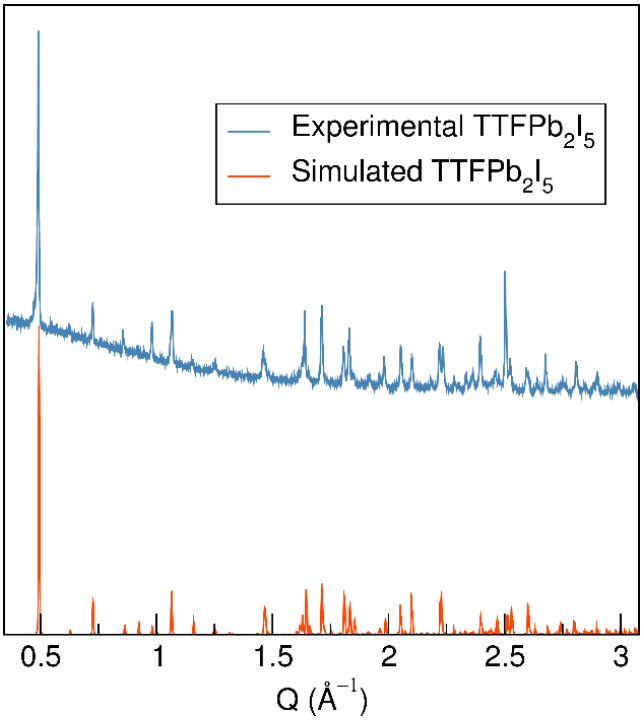

Figure S2. PXRD of (TTF)Pb_2I_5 bulk sample and the simulation of pattern shown below.

Crystallographic information

Single Crystal X-ray diffraction data for (TTF)Pb_2I_5 was collected on a Bruker KAPPA APEX II diffractometer equipped with an APEX II CCD detector using a TRIUMPH monochromator with a Mo Kα X-ray source (α = 0.71073 Å). The crystals were mounted on a cryoloop under Paratone-N oil and the data reported here was collected at room temperature. Absorption correction of the data was carried out using the multiscan method SADABS.[3] Subsequent calculations were carried out using SHELXTL.[4] Structure determinations were done using direct methods. All hydrogen atom positions were omitted. Structure solution, refinement, and creation of publication materials were performed using SHELXTL. The graphical depiction used in the main paper was done with the program VESTA.[5]

Empirical formula	$(C_6H_4S_4)Pb_2I_5$
Crystal habit, color	Block,red
Crystal size (mm)	0.05 × 0.05 × 0.025

Crystal system	Monoclinic
Space group	*P* 21/*c*
Vol (Å)	2048(6)
a	12.90(3)
b	7.97(1)
c	20.23(2)
α	90
β	100.25
γ	90
Z	4
fw (g/mol)	1249.18
Density (calcd) (g/cm^3)	4.051
Abs coeff (mm^{-1})	24.344
F_{ooo}	2116
Total no. reflections	13229
Unique reflections	4124
Final *R* indices [$I > 2\sigma(I)$	R_1 = 0.0643 wR_2 = 0.0872
Largest diff peak and hole (e$^-$ Å^{-3})	1.685 and −1.591
GOF	0.945

Table S1. Crystallographic information for (TTF)Pb_2I_5 single crystal analysis performed at room temperature

4-Probe Conductivity Measurement Setup

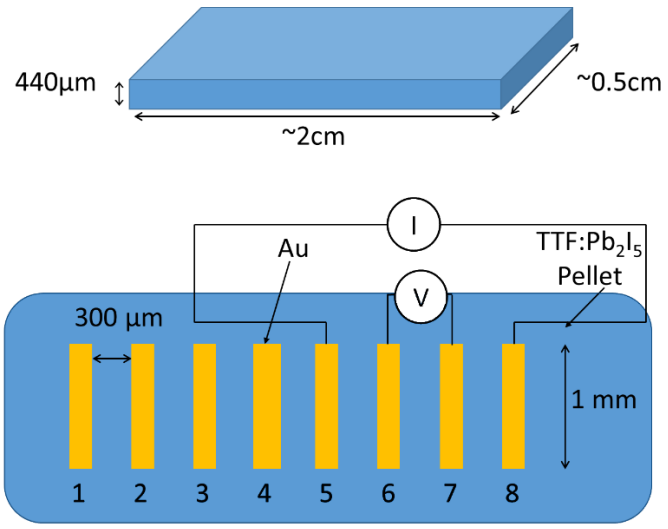

Figure S3. Cartoon depiction of the 4-probe setup employed for the IV measurements. Gold contacts were evaporated onto a pressed pellet of (TTF)Pb_2I_5, and contacts 5 – 8 proved most reliable for measurements. These were wired, and utilized in the reported measurements according to the above schematic.

$TTFI_3$ Band Structure

The computational methods that were employed for the simulation of $(TTF)Pb_2I_5$, which are described in the main body of the manuscript, were also used to acquire the band structure calculations for $TTFI_3$.

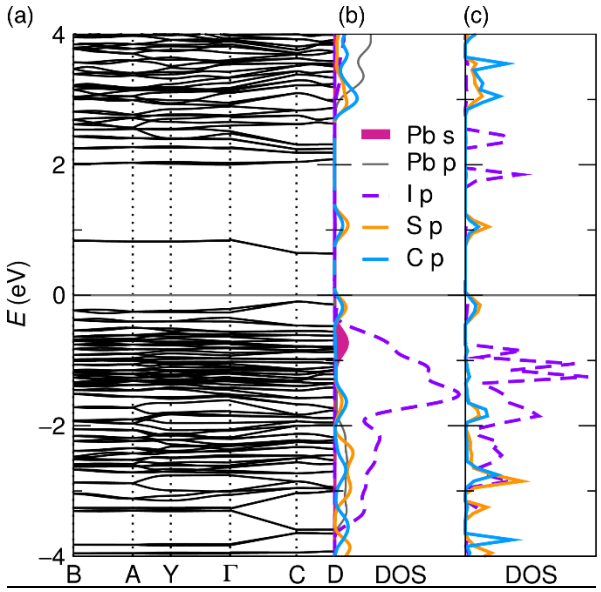

Figure s4: (a) Band structure (PBE) and (b) partial DOS (HSE) of (TTF)Pb2I5. The calculated band gap (HSE: 1.02 eV) is indirect between the special *k*-points C in the valence band and D in the conduction band. (c) Partial DOS of the triiodide $(TTF)I_3$ for comparison. The Fermi energy level is represented as a horizontal line.

Easy Spin Simulation[6]

The simulation was performed using the pepper function, which is a standard part of Easy Spin. The three *g* tensors reported were utilized as individual values with equal weighting. The crystal space group was included in the calculation as well as the possible angles of position. These angles helped to account for the random orientation of the powder solid-state ESR sample. The angles used were [0 0 0; 0 π/4 0; 0 π/8 0; 0 π/16 0; 0 π/32 0; 0 π/64 0]. A Gaussian broadening was also applied at a value of 0.3 to all *g* tensors.

References:

1. Larson, A. C.; Von Dreele, R. B. "General Structure Analysis System (GSAS)", Los Alamos National Laboratory Report LAUR, **2000**, 86-748
2. Toby, B. H. *EXPGUI*, a graphical user interface for GSAS. *Appl. Cryst.,* **2001,** *34*, 210-213.
3. Sheldrick, G. M. *SADABS* University of Gottingen: Germany, **2005**
4. Sheldrick, G. M. *SHELXTL PC*, Version 6.12; Bruker AXS Inc.: Madison, WI, **2005**
5. Momma, K.; Izumi, F. An integrated three-dimensional visualization system VESTA using wxWidgets. *Commission on Crystallogr. Comput*., **2006**, *7*, 106-119
6. Stoll, S.; Schweiger, A. EasySpin, a comprehensive software package for spectral simulation and analysis in EPR *J. Magn. Reson.,* **2006,** *178(1),* 42-55